Hindawi Publishing Corporation
International Journal of Oceanography
Volume 2013, Article ID 315328, 10 pages
http://dx.doi.org/10.1155/2013/315328

Research Article

Effects of Tidal Range Variability and Local Morphology on Hydrodynamic Behavior and Salinity Structure in the Caeté River Estuary, North Brazil

Geórgenes H. Cavalcante,[1] David A. Feary,[2] and Björn Kjerfve[3]

[1] *Universidade Federal de Alagoas, Instituto de Ciências Atmosféricas, CEP 57072-970, Maceió, AL, Brazil*
[2] *School of the Environment, University of Technology, Sydney, P.O. Box 123, NSW 2007, Australia*
[3] *World Maritime University, P.O. Box 500, S-20 124 Malmö, Sweden*

Correspondence should be addressed to Geórgenes H. Cavalcante; georgenes.cavalcante@icat.ufal.br

Received 12 April 2013; Accepted 18 July 2013

Academic Editor: Renzo Perissinotto

Tidal influence and local morphology on circulation and salt transport are investigated in the Caeté river estuary, a well-mixed estuary along the north coast of Brazil. Velocity, temperature, and salinity data were collected in three different locations along the estuary's main channel, over three single, 13 h tidal cycles. The aim of this study was to investigate the relationship between tidal distortion and salinity by using classical methods of comparison of three cross-channel circulation characteristics, as well as computation of salt flux and vertical mixing. Findings indicate a flood-ebb asymmetry in currents, due to the distinct funneling morphology of the estuary, with shallow marginal areas being dominant towards the estuary head, while both stratification and shear dominate near the estuary mouth. The tidal currents enhanced vertical diffusion in the mid- and lower reaches, explaining the prevailing weakly stratified conditions, while the dominant well-mixed conditions in the upper estuary are a result of a combination of stronger flood currents and negligible vertical saline gradient. The predominant downstream salt transport supports the conclusion that there is little accumulation of salt in the Caeté river estuary. In addition, findings indicate that tidal correlation and Stokes drift are important components in the upper estuary, while tidal correlation played an important role in the middle estuary, with fluvial discharge most important in the lower estuary.

1. Introduction

The Caeté river estuary system, encompassed within the Pará-Maranhão Basin, forms part of the largest continuous mangrove belt in the world and is characterized by a flat coastal landscape dominated by macrotidal conditions. Within this system the estuarine watercourse is well mixed due to shallow water depth, high tidal amplitude [1], and high current velocities (up to 2 m·s^{-1}) [2]. This mangrove system is of vital importance for nationally important commercial fisheries, especially exploitation of the semi-terrestrial crab (*Ucides cordatus*), which is abundant within inter- and supratidal zones along the Caeté river estuary system. However, despite both the economic and ecological importance of the Caeté river estuary system, as within the majority of estuarine systems in Brazil there is still little information on the dominant physical factors that influence the hydrodynamic processes within this system and consequently little agreement between studies in both total river discharge and drainage area [2, 3].

Macrotides constitute one of the major hydrodynamic forcing agents of estuarine development in northern Brazil [4], with tidal motion being the dominant force in the mixing and suspension of material. Riverine discharge is also an important forcing agent, especially during the northern Brazilian monsoonal season (January to June) [5, 6]. This freshwater discharge is one of the main components of advective salt transport within Brazilian estuarine systems, resulting in low trapping efficiency within these systems [7, 8]. Given the sensitivity to fluvial discharges, salt transport within a system should be measured and interpreted at

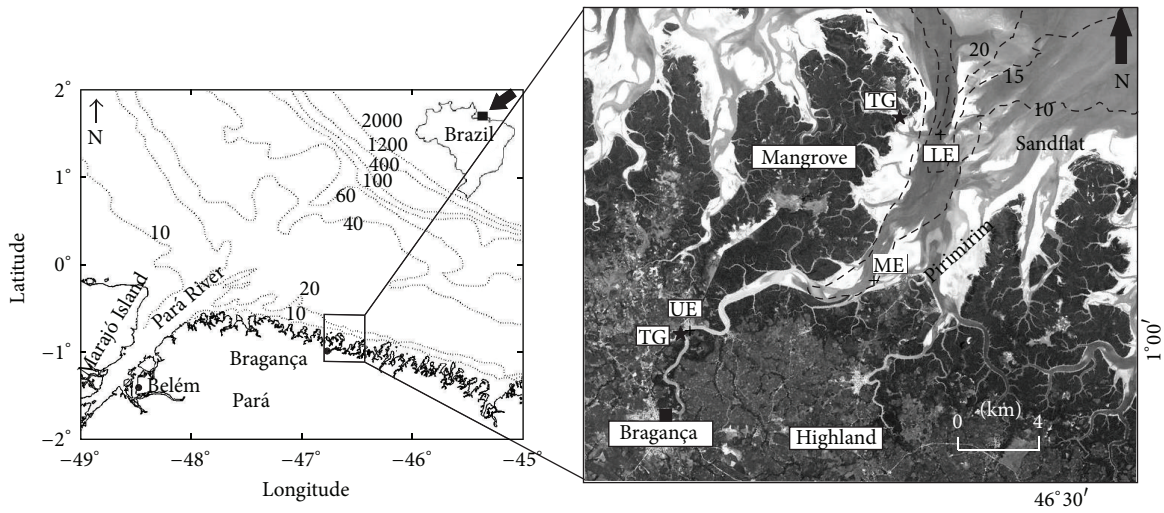

Figure 1: Location of the Caeté river estuary and the oceanographic stations at the upper (UE), middle (ME), and lower (LE) estuarine locations. Location of the two tide gauges (TG) is shown on the map. A demarcation highlighted by a dashed line represents an approximate bathymetry contour in meters along the main-channel and near the adjacent estuary mouth. Mangrove (dark grey tones), highland (light grey tones surrounding Bragança city), and sandflat (white) are also shown on the map.

a uniform cross section, where salt transport mechanisms should be the closest to those addressed in quasi-two dimensional studies [9]. Although we have considered the Caeté estuary as a uniform cross section [10, 11], an estimation of the river discharge was made difficult as 10-11 km from the estuary mouth (see Figure 1) the Caeté river receives discharge from two tributaries, with contributions from smaller creeks flowing in through the mangrove forest. At the time that our measurements were taken, there was no gauging data available for this system, which may potentially lead to an underestimation of water exchange and salt transport in the Caeté river estuary. However, the vast number of studies on estuarine salinity are predominantly concerned with descriptions of salt-transport mechanisms that are based on time-series observations at a small number of stations from a single semidiurnal tidal cycle to several days [12]. Therefore we feel that our measurements of currents and hydrographic properties give a good representation of the physical mechanisms acting in the Caeté river estuary.

Another potential factor that may structure the estuarine hydrodynamic and salt transport in the Caeté estuary is its funnel-shaped geomorphological aspect, which is the result of coastal evolution through mangrove deposits. Transverse shear dispersion becomes more important with increasing width, which is relevant to the divergent morphology towards the Caeté river estuary mouth (which increases in width from 500 m to approximately 7-8 km at its mouth) [13]. Despite the importance of tidal motion, riverine discharge and geomorphology in structuring saline intrusion, and dispersal of other suspended materials within Brazilian estuarine systems [3], there is still little understanding of the mechanisms responsible for salt movement throughout estuarine channels and the factors important in physical forcing (e.g., tides, freshwater flow, wind, etc.) throughout Brazilian estuarine systems [14].

This study investigated the circulation and salt transport characteristics of the Caeté river estuary by examining and comparing spatial variation in water velocity, salinity, and stratification between three different sections within the estuary: the upper or "head," middle, and lower or "mouth" of the estuary. Within each of the three sections we examined (i) tidal propagation, (ii) the degree of stratification and Layer Richardson number, and (iii) the main components of advective salt transport. This is the first attempt to examine the interaction between hydrodynamic conditions and local morphology and to determine their importance in vertical mixing and advective salt transport within the Caeté river estuary. We expected that due to the shape of the estuary (funneled) riverine input would dominate the effects of tidal propagation in structuring both vertical mixing and advective salt transport in the upper estuary. In comparison, the lower estuary was expected to be dominated by tidal propagation, with much less input from riverine sources. Lastly, the equilibrium between both forcing factors (tidal propagation and riverine input) in the mid-estuary was expected to create intermittently vertical salinity stratification.

2. Material and Methods

2.1. Study Area and Field Measurements. The study area forms part of the Caeté Bay system, located 320 km southeast of the Amazon river mouth in northern Brazil (Figure 1). The main geobotanical units in the Bragança coastal plain are made up of mangrove vegetation, with trees reaching up to 20 m (Figure 1—dark grey tones), highlands surrounding Bragança city (light grey), and sandflats (white) [15]. Recent work has estimated that the Caeté river estuary (100 km in length) drains 3,000 km^2 of hinterland, with its discharge varying from 2.8 $m^3 s^{-1}$ to 161 $m^3 s^{-1}$ during dry and rainy seasons, respectively [3]. The regions climate is characterized by

a marked seasonality, with most rainfall occurring between January and June [16]. The experimental period was characterised by below average rainfall (187 mm month^{-1}), with the average monthly rainfall during the experimental time of 230 mm, and an average wind speed of 2.0 ms^{-1} [16]. The wide, funnel-like form of the Caeté river estuary (Figure 1) enables substantial tidal incursion throughout the river system. However, seasonally dependent fluvial discharge maintains relatively low levels of salinity within this system [14].

All data collection was carried out throughout a single spring tidal cycle from 20 to 22 June 2001. Three stations throughout the Caeté river estuary were selected to represent the range of dominant forcing factors potentially important in controlling the mixing and advective transport processes throughout this system. Station selection was also based on the morphology of the Caeté river estuary, so that water parcels sampled at the mooring remained within the well-defined channel of the estuary throughout the tidal cycle, and ensuring a simpler analysis of contributions to the salt transport. The first 10 km of the estuary from the mouth was defined as the lower estuary (LE), where coastal waters were expected to remain during prolonged periods. The mid-estuary (ME) encompassed waters from the LE to 18–20 km upstream and was expected to have reduced halocline stratification than the LE. The upper estuary (UE) encompassed waters from the ME to the upper limit of the coastal salt wedge (estimated to be approximately 40 km from the estuary mouth, based on previous salinity concentration measurements performed during similar conditions [17] (Figure 1)). Sampling in the UE station was undertaken 20-21 June from 13:00 to 01:00, while sampling in the ME station occurred 21-22 June from 14:00 to 02:00 and in the LE station sampling occurred from 10:00 to 22:00 on June 22 (Figure 1).

2.2. Physical and Hydrographical Measurements. The vertical velocity profile of the water column at each station was examined using a single 1200 kHz Workhorse Marine Acoustic Doppler Current Profiler (ADCP: RD Instruments) over one single tidal cycle (13 hours). The ADCP unit was facedown to the side of the ship, with the transducers 0.5 m below the water surface. All measurements were acquired at a vertical resolution of 0.5 m, where each bin consisted of a 5 s average rate of 2 Hz. The ADCP was fixed in space to within the resolution of the internal tilt sensors (<0.01°) and compass (<0.01°). A 10 min averaging window was employed to reduce noise. Vertical profiles of water temperature (°C) and salinity were also recorded every hour with a conductivity, temperature, and depth profiler (CTD: IFM-GEOMAR) during the tidal cycle at each station. Conductivity was measured at a resolution of 0.003 ms cm^{-1}, temperature was measured at a resolution of 0.015°C (with a range of −5 to +35°C), while pressure was measured at a resolution of 0.0025% per metre. Hydrographic properties (temperature, conductivity, and pressure) were converted to salinity (S) and Sigma-t according to the Practical Salinity Scale (PSS-78) and the International Equation of State of Sea Water (IES-80).

Tidal measurements from 23 May to June 30, 2001, were sourced from the Bacuriteua tide gauge (0° 59′ 31″S–46° 44′ 56″W) and the Furo Grande tide gauge (0° 51′ 08″S–46° 37′ 23″W) (Figure 1). The time series of tidal elevation was subjected to harmonic analysis using T_TIDE routines in MATLAB 7.0 [6]. Tidal type was identified by the form-number (Nf), which indicates the ratio of the amplitude of the main diurnal to semidiurnal tidal components $[(K_1 + O_1)/(M_2 + S_2)]$ [18]. Local meteorological data were obtained from the Instituto Nacional de Meteorologia (INMET).

2.3. Current Vectors and Decomposition of the Advective Transport. At each station the current vector was analyzed based on both along (u) and cross-channel (v) components. The Oz axis was oriented upward and its origin was taken on the free surface. The sampling depth (z) was normalized to the nondimensional depth (Z) : $Z = z/h(t)$, where $h(t)$ is the water depth at sampling time [19, 20]. Hydrographic properties (S and T) and the velocity components (u and v) were interpolated along the water column using cubic spline interpolation techniques at intervals of $0.1\,Z$. Extrapolation is the least accurate for the rapidly varying velocity field. In this case, a condition of zero velocity was applied at the bed over the region of extrapolation. Due to the lack of river discharge measurements, the time-depth average of the u-velocity component (u) was taken as an approximate velocity generated by the river discharge.

Due to differences in salinity between tidal cycles, the layer Richardson number (Ri_L) (which takes into account differences in salinity) was used to describe mixing during the tidal cycle based on [8]:

$$\mathrm{Ri}_L = \frac{gh\Delta\rho_v}{\rho\overline{u}^2}, \tag{1}$$

where g is gravity, h is layer depth, $\Delta\rho_v$ is the difference between surface and bottom density, ρ is the averaged density, and u is the longitudinal velocity component. When Ri_L velocity shear is considered sufficient to overcome stratification, and mixing generally occurs; a Ri_L value between 2 and 20 indicates weak stability, with moderate mixing, while $\mathrm{Ri}_L > 20$ indicates strong stability, with turbulent mixing across the stratification largely suppressed [21].

We used the classical stratification-circulation diagram [22] to calculate stratification and circulation parameters for each station. This diagram was also used to classify what type of estuary each station was representing. The components of this diagram ($\Delta S/\langle S\rangle$ and u_s/u_b) were obtained from time-averaged salinity and u-component velocity profiles (surface and bottom) within each station. Within the stratification-circulation diagram v is the key parameter and is defined as the ratio of the tidal correlation term to the total upstream net salt transport term (density-driven + tidal correlation terms) [22]. Salt transport components were described in terms of mean, tidal, steady, and deviation terms according to [23], based on [24, 25]. Considering a laterally homogeneous estuarine cross section, the longitudinal velocity component u can be decomposed as follows:

$$u(x,Z,t) = u_a(x) + u_t(x,t) + u_s(x,Z) + u'(x,Z,t), \tag{2}$$

where u_a is the time- and depth-averaged value given by $\langle \overline{u} \rangle$. The depth-averaged operation is designated by the over bar, and the time-averaged operation is designated by the brackets, which must be averaged over one or more complete tidal cycles. The u_t term represents the variation of the instantaneous depth-averaged velocity along the tidal cycle related to u_a, which is given by $u_t = \overline{u} - u_a$. The u_s term represents the variation of the time-averaged velocity along the water column, which is given by $u_s = \langle u \rangle - u_a$. The primed u' term represents the residuals, which can be attributed to small-scale physical processes and is given by $u' = u - u_a - u_t - u_s$. Similar decomposition can be applied to the salinity, where

$$S(x, Z, t) = S_a(x) + S_t(x, t) + S_s(x, Z) + S'(x, Z, t). \tag{3}$$

Water column thickness (h) will also vary with tide and can also be represented by its variation along the tidal cycle as

$$H(x, t) = h_a + h_t(x, t), \tag{4}$$

where h_a is the time-averaged water depth, given by $\langle h \rangle$, and h_t is the water-level variation along the tidal cycle. The averaged salt transport for one or more tidal cycles (T_s) is given by

$$T_s = \frac{1}{T} \int_0^T \left[\int_0^h \rho u S \, dz \right] dt = \left\langle \overline{\rho u S h} \right\rangle, \tag{5}$$

where ρ is water density, u is longitudinal velocity component, and S is salinity. The substitution of (1) and (2) in (3) results in 32 terms, which produces seven physically significant terms that are nonzero [23]. The seven terms can be attributed to (1) fluvial discharge, (2) Stokes drift, (3) tidal correlation, (4) gravitational circulation, (5) tidal pumping, (6) tidal shear, and (7) long-term drift. The total average salt transport for one or more tidal cycles can therefore be written as follows:

$$T_s = \overline{\rho} \left[u_a S_a h_a + \langle u_t h_t \rangle S_a + \langle u_t S_t \rangle h_a + \overline{u_s} \overline{S_s} h_a + \left\langle \overline{u' S'} \right\rangle h_a + \langle u_t S_t h_t \rangle + u_a \langle S_t h_t \rangle \right]. \tag{6}$$

3. Results

3.1. Tidal Analysis. Harmonic analysis showed that primary tidal forcing within both the UE and LE stations was semidiurnal in nature, with M_2 being the dominant constituent at both stations. At the UE station, the semidiurnal tidal components M_2 and S_2 showed amplitudes of 180 and 54 cm, respectively. These components were overwhelmingly dominant in their relationship with the main diurnal components (K_1: 9.8 cm, O_1: 8.9 cm). Similarly at the LE station, M_2, S_2, K_1, and O_1 were 178, 56, 10, and 10 cm, respectively. The form number of 0.08 was identical for both the UE and LE stations, confirming that the tide along the Caeté river estuary was purely semidiurnal. Within both stations the relative amplitude of the two smaller constituents (S_2 and N_2) to M_2 (S_2/M_2 and N_2/M_2) was 0.28 and 0.19 (UE), and 0.31 and 0.20 (LE), indicating a large spring-neap tide variation. The tidal range did not change significantly between the UE and LE stations (refer to Figure 2); however, tidal phase changed gradually from flood to ebb tides within both stations. The LE leads the phase change by approximately 1 : 45 h (Figure 2), which is indicative of tidal wave distortion within a shallow and sinuous inner estuary (Figure 1).

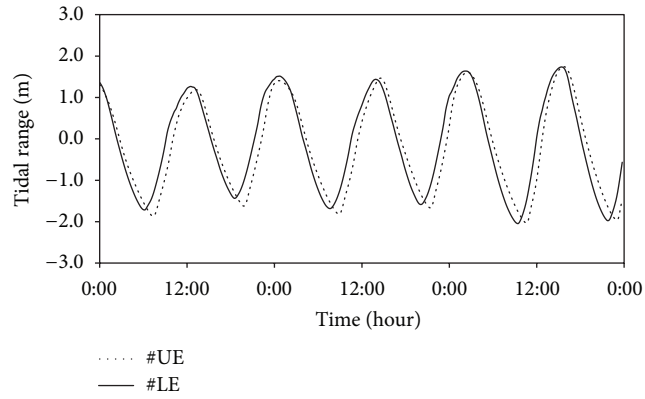

Figure 2: Tide level for upper (UE) and lower (LE) estuaries for the period of 10–12 June 2001.

3.2. Currents and Stratification. The u-component indicated a strong asymmetry between flood ($u < 0$) and ebb ($u > 0$) currents towards the estuary head (UE station), while stratification and shear increased towards the estuary mouth (LE station) (Figure 3). Based on the longitudinal current component (u) the Caeté river estuary can be described as a nonsteady river discharge system that varies in strength toward the estuary head (Figure 3—left panel). Vertical velocity shear was the highest during the flood tide in the UE and ME stations, with high water delaying maximum velocity by approximately 2 h (Figures 3(a) and 3(c)). Vertical shear reached its maximum during the ebb tide in the LE station, with high water leading by almost 2 h current velocity maximum (Figure 3(e)). In general there was a 3 h lag between the vertical averaged salinity contour and the averaged current maximum (Figure 4), indicative of a standing wave tidal regime.

3.3. Vertical Mixing and Estuary Classification. The low Ri_L found at all three stations is indicative of well-mixed conditions. The low temporal variability shows that these well-mixed conditions persist over the tidal cycle (Figure 5). Stratification increases towards the LE station, with increasing Ri_L downstream of the UE and ME stations. Although all three stations alternated between stable and unstable states, an unstable state was the predominant condition found throughout the stations (Figure 5).

All stations can be classified as partially weakly mixed stratified (type 2a) (using the classical stratification-circulation diagram). The key parameter within the diagram (ν)

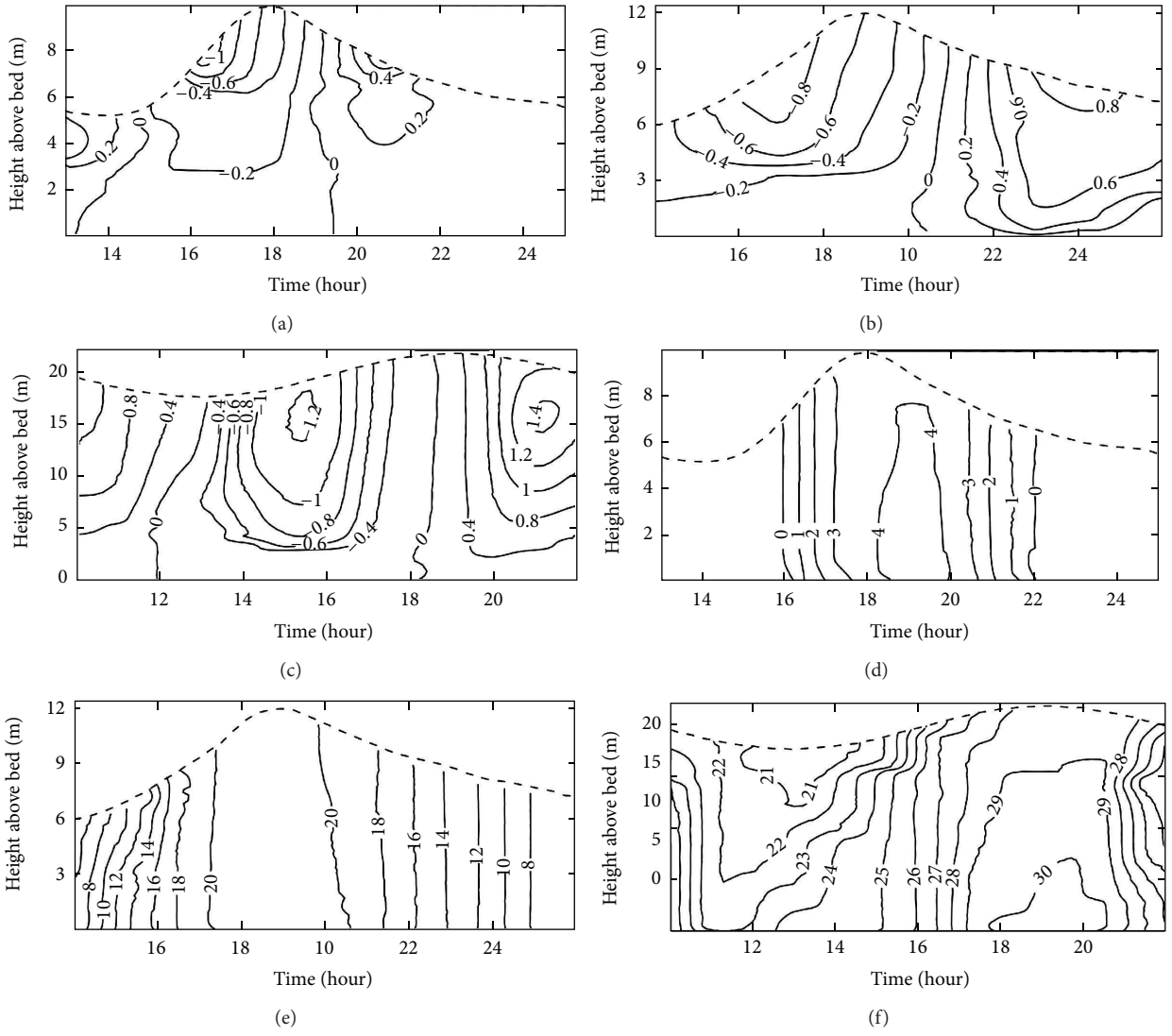

Figure 3: Temporal and vertical variation of the u-component (ms^{-1}) and salinity at the three stations along the Caeté estuary. ((a), (d))—UE; ((b), (e))—ME; ((c), (f))—LE. Positive current speed means downstream and negative means upstream.

ranged from 0.95 to 0.99 (Figure 6), indicating that tidal correlation was responsible for approximately 100% of the upstream salt flux during the tidal cycle, overwhelming any downstream advective flux contribution.

3.4. Salt Transport Components. Although there were pronounced differences in total salt transport between stations, there was little difference in the components important in developing this transport, revealing similar components throughout the stations (Table 1). The total salt transport was negligible at the UE station and riverine discharge contributed the most to the downstream salt transport component. Within the UE station tidal correlation and Stokes drift were dominant components in total upstream salt transport. The ME station showed slightly higher total salt transport than the UE station (Table 1), with any increase in upstream tidal correlation overwhelmed by downstream river discharge and Stokes drift (Table 1). Within the LE station salt transport was dominated by downstream river discharge, while the upstream components (i.e., Stokes drift and tidal correlation) showed comparatively low values (Table 1).

4. Discussion

In parallel with similar estuarine areas within the Amazon River (e.g., [26]), as well as estuarine systems along Brazil's north coast (e.g., [27, 28]), we found that within the Caeté river estuary there was a small reduction in tidal range and a more accentuated phase lag between lower and upper estuarine stations, associated with low frictional and funneling effects within this system [12]. In addition, we also found a small reduction in tidal range and high phase lag towards the estuary head, which is also attributable to the smooth topographical gradient found throughout the system [29].

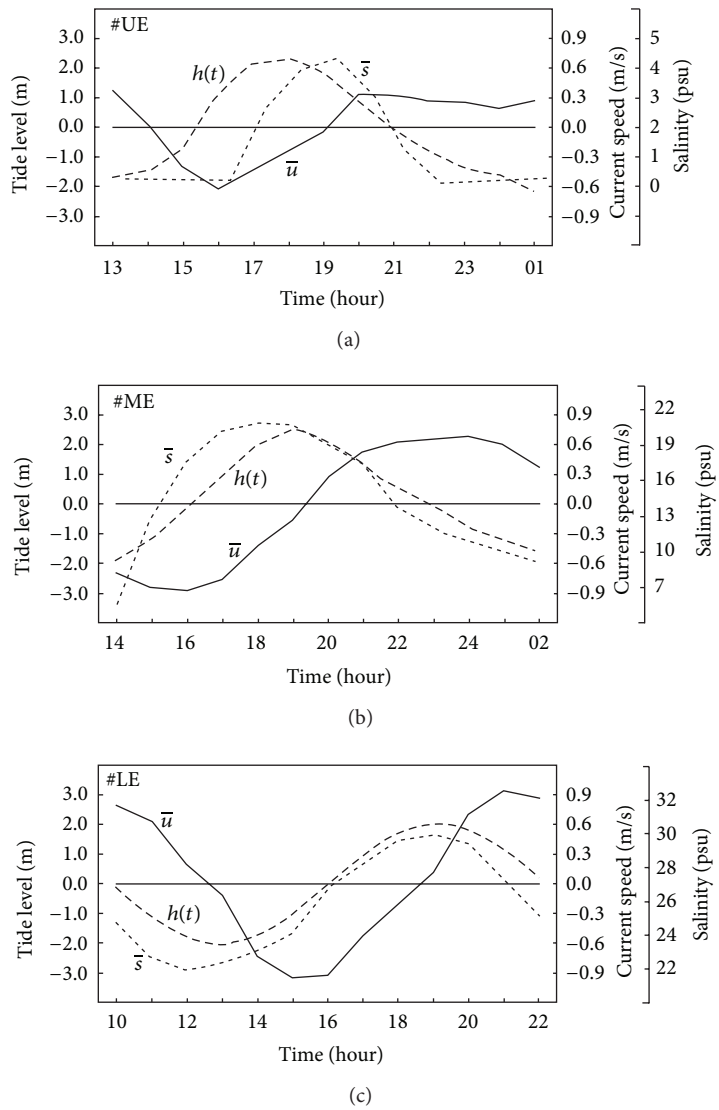

Figure 4: Depth-averaged of along-channel velocities and salinity, and tide level at upper (UE), middle (ME), and lower (LE) estuaries.

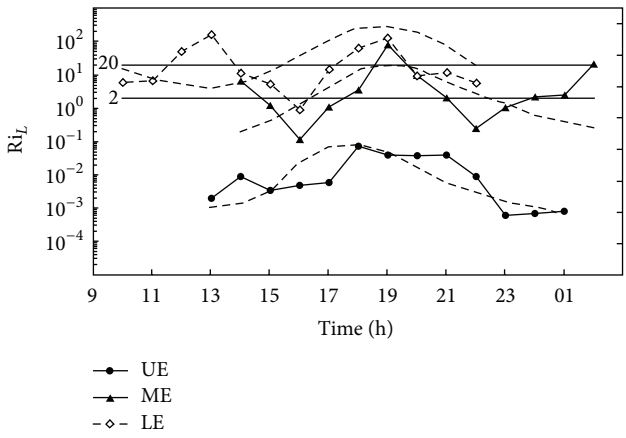

Figure 5: Temporal variation of the layer Richardson number (Ri_L) at upper (UE), middle (ME), and lower (LE) estuaries.

Within a range of estuaries similar to the channel-shoal morphology of the Caeté system (sensu [3]), it has been shown that friction from channel walls may be substantially reduced when $B \gg h$, where B is the width of the main channel [10]. In correspondence, during upstream propagation, tidally driven waves can be substantially modified by friction effects associated with both bed morphology and river width, creating a "funneling" effect [12, 30].

Although the relatively smooth bed topography of the Caeté river estuary minimizes the dampening effect on tidal range, the unique sinuous geometry of the inner Caeté river estuary [17] also contributes to the increased phase lag in upstream tidal wave propagation towards the estuary head [31, 32]. As a result of the Caeté system's geometry, the wave propagation is progressively dampened in this system, suggesting a standing-wave tidal regime within upstream areas [1]. In addition, the strong convergence in river topography

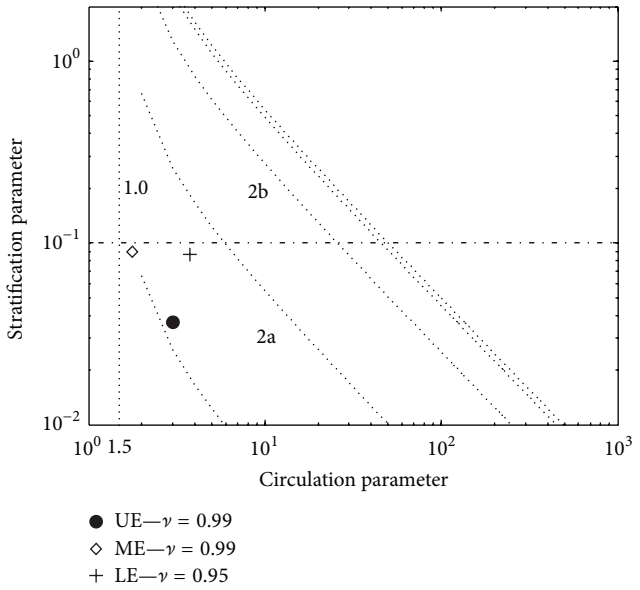

Figure 6: Stratification-circulation diagram for upper (UE), middle (ME), and lower (LE) estuaries. The estuary is classified as Type 2a for all three stations with $\nu = 0.99$, 0.99, and 0.95, respectively.

between the lower and upper estuary (i.e., cross section varies from 8.0 km to approximately 0.2 km from lower to upper estuary) may also alter the nature of tidal propagation within this system (e.g., [9]). Such differences in bed morphology may also explain the longer ebb, than flood tides within the upper estuary [1].

This research showed that there was a significant distortion between flood-ebb currents and salinity distribution along the Caeté river estuary. In general, the flood-ebb asymmetry increased towards the estuary head, while stratification and shear increased towards the estuary mouth, leading to maximum flood velocity exceeding maximum ebb velocity. Such asymmetry in current velocity may be predominantly associated with differences in tidal propagation within tidal cycles [7]. There was faster propagation around high water than low water, which was associated with shorter flood than ebb duration in the upper and mid-estuary [33, 34]. In addition, this asymmetry in current velocity may also be associated with the large tidal flats in the lower section of the Caeté system [29]. This morphological aspect may have contributed to stronger maximum ebb currents in the lower estuary, as large tidal flats can enhance maximum ebb currents. These characteristics are found in estuaries with large tidal flats where lowering of the water level during ebb tide is slower within the flats than adjacent channels [35]. As tidal waves propagate faster in channels than on tidal flats, the increasing current strength during the last stage of the ebb period also increases the net seaward flux of material, as found in the lower estuary station.

There were marginal phase differences between both average current and average salinity and tidal elevation at all three stations. This result supports the prediction that tides in the Caeté river estuary more likely develop a standing oscillation than a progressive wave [36]. Even though the results

Table 1: Summary of salt flux decomposition of advective transport at the lower (# LE), middle (# ME), and upper estuaries (# UE) sampling stations.

Components of advective transport	# UE salt transport ($\mathrm{kg\,m^{-1}\,s^{-1}}$)	# ME salt transport ($\mathrm{kg\,m^{-1}\,s^{-1}}$)	# LE salt transport ($\mathrm{kg\,m^{-1}\,s^{-1}}$)
Fluvial discharge	0.8 ± 0.1	6.0 ± 0.2	22.8 ± 2.2
Stokes drift	−0.4 ± 0.2	4.3 ± 0.1	−3.6 ± 0.3
Tidal diffusion	−0.5 ± 0.3	−9.7 ± 0.6	1.7 ± 0.5
Gravitational circulation	−0.01 ± 0.0	−0.05 ± 0.0	−0.8 ± 0.1
Tidal pumping	0.01 ± 0.0	0.1 ± 0.0	−0.6 ± 0.1
Tidal shear	0.02 ± 0.0	0.2 ± 0.1	0.7 ± 0.1
Residual circulation	0.18 ± 0.0	0.4 ± 0.1	0.2 ± 0.0
Remainder terms	0.0 ± 0.0	0.0 ± 0.0	0.0 ± 0.0
Total transport	0.1 ± 0.2	1.3 ± 0.5	20.4 ± 1.2

showed that the phase difference between tidal elevation and average salinity reduced towards the estuarine mouth where they were in phase, the same did not occur between average current and salinity within the lower estuary, which can be associated with increased along-channel divergence of current close to the estuary mouth [36]. Another factor that affects this divergence in average current and salinity phase is the gradual increase in channel depth from upper to lower estuary, varying from 10 m within the upper and mid-estuary to approximately 22 m towards its mouth [3]. As current speed is sensitive to variation in along-channel bathymetry and small increases in depth will lead to large oscillations in current speeds [37], we can expect that such large increases in depth within the lower estuary will also have substantial effects on the forcing factors important in structuring salt transport within the Caeté river estuary [38].

Counter to our expectations that vertical salinity stratification would be stronger in the middle than upper and lower estuary, there was little evidence of a significant vertical salinity structure within the mid-estuary reaches. In addition, there were little or absent differences in both salinity and temperature between surface and bottom in the mid- and lower estuary, similar to results reported within Caeté inner mangrove creeks [29]. Such low stratification in salinity was associated with high tidal current strength at the benthos, enhancing vertical diffusion leading to a weakly stratified, nearly well-mixed system [39]. With increased tidal forcing, bottom generated mixing strengthens, leading to an increase in the turbulent vertical salt fluxes near the pycnocline [40]. Such turbulence allows fresh water to reach the lower portion of the water column, resulting in stratification breakdown [40]. The close timing of maximum and minimum salinity with HW and LW slack periods in the lower estuary illustrates the overriding importance of tidal advection to the distribution of salinity within the Caeté river estuary [31, 41].

The low values of Ri_L in the upper reaches of the Caeté river estuary indicate that bottom generated mixing (significant tidal mixing) was strong enough to overwhelm buoyancy effects, and mixing was fully developed throughout the tidal cycle [21]. In addition, strong up-estuarine flow revealed

a significant tidal (bed-shear) mixing, reducing the possibility of density current formation and pronounced stratification [8]. Although the vertical saline structure within the mid- and lower estuary indicated nearly well-mixed conditions, the Ri_L moved between weak-stability limits (i.e., $Ri_L = 2$ and 20) during the ebb tide and associated slower tidal current speeds. The strong stability ($Ri_L > 20$) found in the lower estuary can be explained by the reduction in current flow (slack tide), which effectively enhances vertical stratification [5, 42]. Such vertical stratification will be important in ecosystem development within the Caeté river estuary, as stratification reduces vertical mixing and vertical flux in ecologically important variables such as phytoplankton, heat, and nutrients [2].

The dominant downstream advective salt transport at all three stations suggests that there is little salt accumulation inside the Caeté river estuary and that there is a predominance of riverine input in material exchange, especially near the estuary mouth. These findings disagree in part with our initial prediction that advective salt transport would be dominated by riverine input in the upper estuary and density-driven current in the lower estuary. There was an asymmetry in the duration of the rise and fall of water level and changes in asymmetry between flood and ebb currents relative to the slack current ($u = 0$). Such asymmetry in rise and fall of water level led to a residual current directed down-estuary in the upper and mid-estuary, while classical (although weak) gravitational circulation was apparent in the lower estuary. In addition, the longer ebb duration in the upper and mid-estuary dominated flood currents, contributing to the predominant downstream salt transport. In comparison, the strong currents during the last stage of the ebb period in the lower estuary led to an ocean-ward net outflow, responsible for 89% of the net salt transport within this section of the estuary.

The present work showed that both Stokes drift and tidal correlation played substantially dissimilar roles in downstream and upstream salt transport, similar to salt transport studies on large estuaries [23, 43]. This result is different to that found in other estuaries, where estuarine salt transport and vertical shear dispersion have been found to be the dominant mechanism driving down-gradient salt flux [9, 20]. Theoretically, Stokes drift should be influencing upstream salt transport, while tidal dispersion is expected to be the predominant factor in controlling downstream salt transport [44]. However, the importance of Stokes drift within the Caeté river estuary system can be explained by the shorter but stronger flood currents in the upper estuary, and a longer flood current in the lower estuary, suggesting that these factors counteracted and even dominated Stokes drift [1]. In addition, tidal correlation remained upstream in both upper and mid-estuary reaches, counteracting the predominant downstream salt transport. The importance of tidal correlation in structuring salt transport in the mid-estuary may also be attributed to the longer periods of upstream current within this section, where salt remained for up to 2 hrs after high tide. These two salt transport terms (i.e., Stokes drift and tidal correlation) were masked by the stronger fluvial input in the lower estuary, minimizing both transport terms in affecting total net change in salt transport.

Within the Caeté system both gravitational circulation and tidal pumping play a small role in the upstream salt transport in the lower estuary and are almost negligible in the mid- and upper estuary reaches. This differential importance of both transport terms between estuary sections may be attributed to several features of the estuary: (i) the distortion in upstream tide propagation towards the estuarine head, (ii) asymmetry in flood and ebb currents at all the stations, (iii) weak salinity stratification in upper and mid-estuary reaches, and (iv) increased stratification towards the estuary mouth. Similar results have also been observed by [43, 45], where such variability in salt terms was attributed to distortion in tide propagation and weak vertical stratification. Considering the small magnitude in salt transport, long-term drift played an important role in the upper estuary, with increased residual circulation and lowered upstream mass transport by Stokes drift and tidal correlation showing that this section was at the limit of coastal salt intrusion.

The distribution of salt throughout an estuarine system (i.e., Caeté river estuary) is the integrated history of salt transport and does not necessarily reflect the magnitude of salt transport at the time of the measurement [11, 46]. Overall, both salt transport and salinity stratification at all three stations were strongly dependent on fluvial discharge, with tidal range being substantially less important. There was considerable unsteadiness in the salt balance at all three locations, as shown by variability in advective and dispersive salt fluxes, also described in other estuarine studies [32, 47]. This research found that as a consequence of the unbalanced advective and dispersive salt components, the rate of change in salt content was comparable to the magnitude of individual flux terms, with net salt transport in the lower estuary. Perhaps the most interesting question to be further investigated is what sets the strong downstream salt transport in the lower estuary relative to the other sections. Overall, we believe that the present research represents a substantial step in understanding the spatial differences in hydrodynamic and correspondent salt transport within the Caeté river estuary. Further work should include longer temporal recording and a higher number of sampling stations throughout this system, to more completely examine the influence of morphology and hydrodynamics in salt transport mechanism along the Caeté river estuary.

5. Conclusions

We found that there is a relatively small reduction in tidal range from the lower to the upper reaches of the Caeté river estuary system, and that this is attributed to the smooth topographical gradient found in the Bragança mangrove areas. Such a reduced effect of tidal movement within the upper estuary is also predicted to be due to the frictional effect of the convergent and sinuous inner topography throughout this system. Within this system, the flood-ebb asymmetry in currents increases towards the upper reaches of the estuary, while stratification and shear increased towards lower reaches. The tidal current was the main determining agent for enhancing vertical diffusion in the mid- and lower estuary, where the Ri_L distribution presented stable and unstable

conditions reflected in weakly stratified, nearly well-mixed conditions. In the upper estuary, stronger flood currents were also observed, but the vertical saline gradient was negligible and low Ri_L persisted over the tidal cycle with relatively well-mixed conditions prevailing. The dominant down-estuary flow at all stations was due to correlation between longer ebb tide and tidally averaged residual current downstream. The predominant downstream transport of salt was dominated by river discharge at all three stations, with Stokes drift also presenting a net downstream in the middle estuary. The upstream transport of salt was dominated by tidal correlation and Stokes drift in the upper estuary, while in the mid-estuary, only tidal correlation plays a role in salt transport. The net downstream salt transport in the lower estuary was comparable to the magnitude of the individual downstream fluvial discharge term, with the remaining components only of marginal importance. The study also reveals the inherent unsteadiness of the salt balance over the specific experiment which requires further investigation to identify the range of flux mechanisms in a variety of spring-neap cycles.

Acknowledgments

This work was carried out as part of the doctorate thesis of Geórgenes H. Cavalcante, with support from the Federal University Fluminense. This paper resulted from the cooperation between the Center for Tropical Marine Ecology (ZMT), Bremen, Germany and the Universidade Federal do Pará (UFPa), Belém, Brazil, under the Governmental Agreement on Cooperation in the Field of Scientific Research and Technological Development between Germany and Brazil. Thanks are due to CAPES and to FAPERJ for research grants to Geórgenes H. Cavalcante and to Texas A&M University for infrastructure support. David A. Feary was supported by a Chancellors Postdoctoral Fellowship within the University of Technology, Sydney. The authors are also indebted to the anonymous reviewers for their judicious remarks and fruitful suggestions. This is a MADAM contribution which has been financed by the German Ministry for Education, Science, Research and Technology (BMBF) [Mangrove Management and Dynamics-MADAM], and the Conselho Nacional de Pesquisa e Tecnologia (CNPq).

References

[1] J. Dronkers, "Tidal asymmetry and estuarine morphology," *Netherlands Journal of Sea Research*, vol. 20, no. 2-3, pp. 117–131, 1986.

[2] R. J. Uncles, J. E. Ong, and W. K. Gong, "Observations and analysis of a stratification-destratification event in a tropical estuary," *Estuarine, Coastal and Shelf Science*, vol. 31, no. 5, pp. 651–665, 1990.

[3] G. H. Cavalcante, *Oceanographic processes in the coastal and estuarine region of the Caeté River, Pará [Ph.D. dissertation]*, Federal University Fluminense, 2007.

[4] R. C. Beardsley, J. Candela, R. Limeburner et al., "The M2 tide on the Amazon shelf," *Journal of Geophysical Research*, vol. 100, no. 2, pp. 2283–2319, 1995.

[5] D. K. Ralston and M. T. Stacey, "Stratification and turbulence in subtidal channels through intertidal mudflats," *Journal of Geophysical Research C*, vol. 110, no. 8, Article ID C08009, pp. 1–16, 2005.

[6] R. Pawlowicz, B. Beardsley, and S. Lentz, "Classical tidal harmonic analysis including error estimates in MATLAB using TDE," *Computers and Geosciences*, vol. 28, no. 8, pp. 929–937, 2002.

[7] A. J. F. Hoitink, P. Hoekstra, and D. S. Van Maren, "Flow asymmetry associated with astronomical tides: implications for the residual transport of sediment," *Journal of Geophysical Research C*, vol. 108, no. 10, article 3315, 2003.

[8] K. R. Dyer and A. L. New, "Intermittency in estuarine mixing," in *Estuarine Variability*, D. A. Wolfe, Ed., pp. 321–339, Academic Press, 1986.

[9] M. M. Bowen and W. R. Geyer, "Salt transport and the time-dependent salt balance of a partially stratified estuary," *Journal of Geophysical Research C*, vol. 108, no. 5, article 3158, 2003.

[10] C. T. Friedrichs and D. G. Aubrey, "Non-linear tidal distortion in shallow well-mixed estuaries: a synthesis," *Estuarine, Coastal and Shelf Science*, vol. 27, no. 5, pp. 521–545, 1988.

[11] J. R. West and J. S. Mangat, "The determination and prediction of longitudinal dispersion coefficients in a narrow, shallow estuary," *Estuarine, Coastal and Shelf Science*, vol. 22, no. 2, pp. 161–181, 1986.

[12] D. Prandle, "Relationships between tidal dynamics and bathymetry in strongly convergent estuaries," *Journal of Physical Oceanography*, vol. 33, pp. 2738–2750, 2003.

[13] P. W. M. Souza-Filho, G. C. Lessa, M. C. L. Cohen, F. R. Costa, and R. J. Lara, "The Subsiding macrotidal barrier estuarine system of the Eastern Amazon Coast, Northern Brazil," in *Geology and Geomorphology of Holocene Coastal Barriers of Brazil*, S. F. Dillenburg and P. A. Hesp, Eds., vol. 107 of *Lecture Notes in Earth Sciences*, pp. 347–376, Springer, New York, NY, USA, 2009.

[14] L. Schwendenmann, *Tidal and seasonal variations of soil and water properties in a Brazilian mangrove ecosystem [M.S. thesis]*, University of Karlsruhe, Resources Engineering Programme, 1998.

[15] P. W. M. Souza Filho, E. D. S. Farias Martins, and F. R. da Costa, "Using mangroves as a geological indicator of coastal changes in the Bragança macrotidal flat, Brazilian Amazon: a remote sensing data approach," *Ocean and Coastal Management*, vol. 49, no. 7-8, pp. 462–475, 2006.

[16] INMET, *Normas Climatológicas (1961–1990)*, Instituto Nacional de Meteorologia, Brasilia, Brazil, 1992.

[17] G. H. Cavalcante, B. Kjerfve, B. Knoppers, and D. A. Feary, "Coastal currents adjacent to the Caeté Estuary, Pará Region, North Brazil," *Estuarine, Coastal and Shelf Science*, vol. 88, no. 1, pp. 84–90, 2010.

[18] A. Defant, *Physical Oceanography*, vol. 2, Pergamon Press, New York, NY, USA, 1960.

[19] B. Kjerfve, "Velocity averaging in estuaries characterized by a large tidal range to depth ratio," *Estuarine and Coastal Marine Science*, vol. 3, no. 3, pp. 311–323, 1975.

[20] J. A. Lerczak, W. R. Geyer, and R. J. Chant, "Mechanisms driving the time-dependent salt flux in a partially stratified estuary," *Journal of Physical Oceanography*, vol. 36, no. 12, pp. 2296–2311, 2006.

[21] L. B. Miranda, A. L. Bérgamo, and C. A. Ramos e Silva, "Dynamics of a tropical estuary: curimataú river, NE Brazil," in *Proceedings of the 8th International Coastal Symposium*, Expanded Abstract, Itajaí, Brazil, 2004.

[22] D. V. Hansen and M. Rattray, "New dimensions in estuary classification," *Limnology and Oceanography*, vol. 11, pp. 319–325, 1966.

[23] L. B. Miranda, B. M. Castro, and B. Kjerfve, *Princípios de Oceanografia Física de estuários*, EDUSP, S. Paulo, Brazil, 2002.

[24] K. F. BOWDEN, "The mixing processes in a tidal estuary," *Air and Water Pollution*, vol. 7, pp. 343–356, 1963.

[25] K. Hunkins, "Salt dispersion in the hudson estuary," *Journal of Physical Oceanography*, vol. 11, pp. 729–738, 1981.

[26] P. Kosuth, J. Callède, A. Laraque et al., "Sea-tide effects on flows in the lower reaches of the Amazon River," *Hydrological Processes*, vol. 23, no. 22, pp. 3141–3150, 2009.

[27] B. Kjerfve and H. O. Ferreira, "Tidal bores: first ever measurements," *Ciência e Cultura*, vol. 45, no. 2, pp. 135–138, 1993.

[28] V. F. Santos, A. G. Figueiredo Jr, O. F. M. Silveira et al., "Processos Sedimentares em áreas de macro-marés influenciados pela pororoca—estuário do rio Araguari-Amapá-Brasil," in *Congressso da Associação Brasileira de Estudos do Quaternário, ABEQUA*, Artigos, Guarapari, Brazil, 2005.

[29] M. C. L. Cohen, R. J. Lara, J. F. F. Ramos, and T. Dittmar, "Factors influencing the variability of Mg, Ca and K in waters of a mangrove creek in Braganca, North Brazil," *Mangroves and Salt Marshes*, vol. 3, no. 1, pp. 9–15, 1999.

[30] K. R. Dyer, "Sediment transport processes in estuaries," in *Geomorphology and Sedimentology of Estuaries*, G. M. E. Perillo, Ed., pp. 423–449, Elsevier, New York, NY, USA, 1995.

[31] J. H. Simpson, J. Brown, J. Matthews, and G. Allen, "Tidal straining, density currents, and stirring in the control of estuarine stratification," *Estuaries*, vol. 13, no. 2, pp. 125–132, 1990.

[32] J. H. Simpson, R. Vennell, and A. J. Souza, "The salt fluxes in a tidally-energetic estuary," *Estuarine, Coastal and Shelf Science*, vol. 52, no. 1, pp. 131–142, 2001.

[33] R. A. Heath, "Phase relations between the over- and fundamental-tides," *Deutsche Hydrographische Zeitschrift*, vol. 33, no. 5, pp. 177–191, 1980.

[34] R. J. Uncles, "A note on tidal asymmetry in the severn estuary," *Estuarine, Coastal and Shelf Science*, vol. 13, no. 4, pp. 419–432, 1981.

[35] J. D. Boon III and R. J. Byrne, "On basin hyposmetry and the morphodynamic response of coastal inlet systems," *Marine Geology*, vol. 40, no. 1-2, pp. 27–48, 1981.

[36] J. N. Hunt, "Tidal oscillations in Estuaries," *Geophysical Journal International*, vol. 8, no. 4, pp. 440–455, 1964.

[37] D. B. Chadwick and J. L. Largier, "The influence of tidal range on the exchange between San Diego Bay and the ocean," *Journal of Geophysical Research C*, vol. 104, no. 12, pp. 29885–29899, 1999.

[38] J. F. Festa and D. V. Hansen, "Turbidity maxima in partially mixed estuaries: a two-dimensional numerical model," *Estuarine and Coastal Marine Science*, vol. 7, no. 4, pp. 347–359, 1978.

[39] G. J. de Boer, J. D. Pietrzak, and J. C. Winterwerp, "On the vertical structure of the Rhine region of freshwater influence," *Ocean Dynamics*, vol. 56, no. 3-4, pp. 198–216, 2006.

[40] M. L. Becker, R. A. Luettich, and H. Seim, "Effects of intratidal and tidal range variability on circulation and salinity structure in the Cape Fear River Estuary, North Carolina," *Journal of Geophysical Research C*, vol. 114, no. 4, Article ID C04006, 2009.

[41] S. Monismith, J. R. Burau, and M. Stacey, "Stratification dynamics and gravitational circulation in northern San Francisco Bay," in *San Francisco Bay: The Ecosystem*, J. T. Hollibaugh, Ed., pp. 123–153, AAAS Press, 1996.

[42] D. K. Ralston and M. T. Stacey, "Longitudinal dispersion and lateral circulation in the intertidal zone," *Journal of Geophysical Research C*, vol. 110, no. 7, pp. 1–17, 2005.

[43] L. B. de Miranda, A. L. Bérgamo, and B. M. de Castro, "Interactions of river discharge and tidal modulation in a tropical estuary, NE Brazil," *Ocean Dynamics*, vol. 55, no. 5-6, pp. 430–440, 2005.

[44] H. B. Fischer, E. J. List, R. C. Y. Koh, J. Imberger, and N. H. Brooks, "Mixing in inland and coastal waters," 1979.

[45] R. J. Uncles and J. A. Stephens, "The effects of wind, runoff and tides on salinity in a strongly tidal sub-estuary," *Estuaries and Coasts*, vol. 34, no. 4, pp. 758–774, 2011.

[46] D. A. Jay, R. J. Uncles, J. Largier, W. R. Geyer, J. Vallino, and W. R. Boynton, "A review of recent developments in estuarine scalar flux estimation," *Estuaries*, vol. 20, no. 2, pp. 262–280, 1997.

[47] N. S. Banas, B. M. Hickey, P. MacCready, and J. A. Newton, "Dynamics of Willapa Bay, Washington: a highly unsteady, partially mixed estuary," *Journal of Physical Oceanography*, vol. 34, no. 11, pp. 2413–2427, 2004.